Chemistry—Methods

Research Article
doi.org/10.1002/cmtd.202200060

Chemistry Europe
European Chemical Societies Publishing

www.chemistrymethods.org

In Silico Design of Dihydroazulene/Vinylheptafulvene Photoswitches for Solar-Energy Storage Guided by an All-Around Performance Descriptor**

Enrique M. Arpa* and Bo Durbeej*[a]

A major challenge in the development of molecular photoswitches capable of storing and releasing solar energy is to simultaneously realize many of the performance criteria required of the switches for such applications. Here, we take on this challenge by introducing an all-around performance descriptor that combines three key criteria (related to energy density, storage time and light-absorption characteristics), and by using density functional theory methods to calculate its values for 52 newly designed dihydroazulene/vinylheptafulvene (DHA/VHF) switches. Thereby, we are able to identify several switches with excellent overall properties that contain a structural motif absent in all DHA/VHF compounds previously considered for solar-energy storage. For some of these switches, we also provide retrosynthetic analyses and demonstrate that they form the energy-storing VHF isomer through a facile DHA→VHF photoisomerization reaction. All in all, we conclude that these switches show great promise for further development towards applications in solar-energy storage.

Introduction

The ever-increasing demand for sustainable energy solutions continues to trigger research into new materials for exploiting the energy that our sun inexhaustibly provides. Among molecular-based materials, various types of molecular photoswitches are of particular interest in light of well-known challenges to account for the variation in both solar influx and energy demand with the time of day, the weather and the season. Specifically, certain molecular photoswitches are able to store absorbed solar energy as chemical energy through their associated photochemical conversion into energy-rich, yet stable, isomeric forms.[1–3] When the absorbed solar energy subsequently is needed, these isomeric forms are made (catalytically) to return to their parent forms through a thermal back-reaction, whereby the excess of chemical energy is released as heat. Synthetic photoswitches tailor-made for this particular function are often referred to as molecular solar thermal energy (MOST) systems.[4,5]

For the design of an efficient MOST system, two thermochemical properties are of special interest. One is the (gravimetric) energy-storage density ($\Delta G_{storage}$), which measures the free-energy difference between the photoproduct isomer and the parent isomer per unit weight, and thus indicates how much solar energy can be stored as chemical energy by the MOST system in question. Another is the activation free energy for the thermal back-reaction ($\Delta G^{\ddagger}$), which reflects how quickly the photoproduct isomer will revert to the (more stable) parent isomer in the absence of a catalyst, or, differently put, how long the solar energy can be stored. Generally, for an efficient MOST system, it is commonly accepted that the values of $\Delta G_{storage}$ and $\Delta G^{\ddagger}$ should exceed 0.30 MJ kg^{-1} and 100 kJ mol^{-1},[2,6] respectively.

Besides the aforementioned thermochemical properties, certain photophysical and photochemical characteristics are also deemed desirable for a MOST system, such as a high quantum yield for the forward photoisomerization and an inertness towards photochemical side-reactions (e.g., photodegradation) that compete with the switching between the two isomers. Furthermore, the photoactive isomer should have a UV-vis absorption spectrum that is centered in the violet-blue regime, in which both the solar irradiance at the Earth's surface and the photon energy are sufficiently high to facilitate efficient photoconversion.[2] Moreover, this spectrum should mismatch as much as possible with that of the photoproduct isomer, so that both species absorb maximally at a unique wavelength.[2,3,5] This is to ensure that the photoactive isomer does not have to compete with the photoproduct for light absorption, and to prevent the latter species from hampering the forward photoisomerization. However, despite its importance, the degree of spectral mismatch is rarely quantified or even considered in the design of MOST systems.

To date, several different core structures have been utilized for the development of MOST systems. These structures are typically low-weight organic molecules that, upon light absorption, undergo either cycloaddition, double-bond isomerization

[a] Dr. E. M. Arpa, Prof. B. Durbeej
Division of Theoretical Chemistry, IFM
Linköping University
581 83 Linköping (Sweden)
E-mail: enrique.arpa@liu.se
bodur@ifm.liu.se

[**] A previous version of this manuscript has been deposited on a preprint server (https://doi.org/10.26434/chemrxiv-2022-zjsrb).

Supporting information for this article is available on the WWW under https://doi.org/10.1002/cmtd.202200060

© 2023 The Authors. Published by Wiley-VCH GmbH. This is an open access article under the terms of the Creative Commons Attribution Non-Commercial NoDerivs License, which permits use and distribution in any medium, provided the original work is properly cited, the use is non-commercial and no modifications or adaptations are made.

© 2023 The Authors. Published by Wiley-VCH GmbH

26289725, 0, Downloaded from https://chemistry-europe.onlinelibrary.wiley.com/doi/10.1002/cmtd.202200060 by Linkoping Universitet, Wiley Online Library on [03/04/2023]. See the Terms and Conditions (https://onlinelibrary.wiley.com/terms-and-conditions) on Wiley Online Library for rules of use; OA articles are governed by the applicable Creative Commons License

or electrocyclic reactions. Among them, perhaps the norbornadiene/quadricyclane system, in which the former species produces the latter, highly strained species through a [2 + 2] cycloaddition, has been developed the furthest.[7–13] Other systems include azobenzene,[14–18] dithienylethene,[19–22] and fulvalene ruthenium[23–26] compounds. More recently, 1,2-azaborines have been brought into consideration for MOST applications, owing to their ability to photoisomerize into strained, Dewar-like structures.[27]

Another commonly explored core structure in this field of research is the dihydroazulene/vinylheptafulvene (DHA/VHF) system shown in Figure 1. Upon irradiation, the C_1–C_{8a} bond of DHA is cleaved to form VHF through an electrocyclic ring opening.[28] The first DHAs synthesized and tested for MOST applications had two cyano groups at C_1 and a phenyl ring at C_2, which was either unsubstituted or monosubstituted at the *para* position.[29,30] However, despite exhibiting reasonable photoisomerization quantum yields (0.58 at best), the small $\Delta G_{storage}$ values (0.11 MJ kg^{-1}) and short half-lives (3 h) of the corresponding VHF isomers meant that the room for improvement was ample.

Subsequently, Hammett correlation studies showed that an electron-withdrawing group is needed at C_1 for the thermal back-reaction (VHF→DHA) to take place, due to the associated stabilization of a negative charge in the zwitterionic transition state.[31,32] However, while a DHA compound bearing a single cyano group at C_1 achieved an improved $\Delta G_{storage}$ value, its back-reaction did not proceed.[33] Interestingly, this cyano group could be replaced by other substituents, such as amides, imidates or ketones, without impairing the photochemical reactivity of the DHA isomer.[34] Furthermore, placing an additional cyano group at C_7 allowed the back-reaction to proceed, but $\Delta G_{storage}$ remained small (0.10 MJ kg^{-1}).[35] While benzannulation at different positions increased $\Delta G_{storage}$ by shifting the aromatic/antiaromatic balance between the two isomers, this approach also resulted in the formation of unstable VHFs and triggered photochemical side-reactions.[36,37]

One of the reasons for the small $\Delta G_{storage}$ values of the aforementioned DHA/VHF systems is the tendency of the s-*cis* VHF isomer produced by the ring opening to release steric strain through a rotation of the C_2–C_3 bond, which forms the s-*trans* VHF isomer. Therefore, several attempts have been made to introduce a "conformational lock" in the structure, so as to maintain s-*cis* VHF. Different saturated and/or unsaturated bridges have been tested, linking the C_3 atom with an *ortho* phenyl group placed at C_2.[38,39] While improved $\Delta G_{storage}$ values of around 0.4 MJ kg^{-1} were obtained, this strategy also brought about an undesirable lowering of the $\Delta G^{\ddagger}$ values.[38,39] As for other developments, DHA/VHF systems that incorporate two DHA subunits in a macrocycle have also been realized, whereby the thermal back-reaction proceeds in two steps on a fast (VHF-VHF→DHA-VHF) and a slow (DHA-VHF→DHA-DHA) timescale, respectively.[40–42] In order to trigger this reaction, Nielsen and coworkers showed that Cu(I) is a potent catalyst applicable to both free and macrocyclic DHA/VHF systems.[43] That same year, a catalytic flow reactor for this purpose was developed, alongside a photoconversion device for using the DHA/VHF couple to collect solar energy under outdoor conditions.[44]

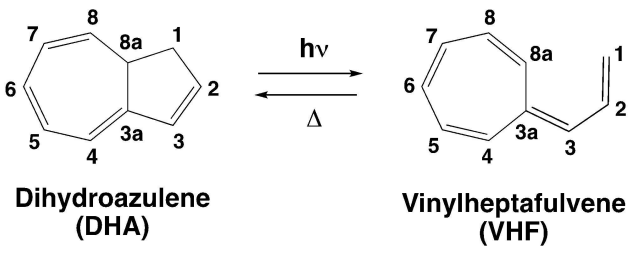

Figure 1. Structure and atom numbering of the dihydroazulene/vinylheptafulvene MOST system.

Various aspects of the DHA/VHF couple that are central to its use as a MOST system have also been investigated by computational methods. For example, regarding the mechanism of the DHA→VHF photoconversion, it has been shown that DHA becomes planar upon excitation to the lowest singlet excited state (S_1) and that the formation of VHF is mediated by internal conversion to the ground state (S_0) within ~600 fs.[45,46] In other studies, Mikkelsen and coworkers have identified suitable density functional theory (DFT) methods for calculating optical and thermochemical properties of DHA/VHF systems,[47] and used such methods to predict how different electron donating or withdrawing groups influence the $\Delta G_{storage}$ values.[48] Despite these efforts, there seems to be no studies in the literature where computational methods are used in a "bottom-up" way to design DHA/VHF compounds that fulfill as many key performance criteria as possible within one and the same molecular framework. Rather, most computational studies of DHA/VHF compounds have focused on properties of already synthesized molecules.[34–37,39–41] This contrasts with the situation for other MOST systems like the norbornadiene/quadricyclane couple, for which bottom-up designs have indeed been reported.[49,50] Accordingly, there is a need to better exploit well-known advantages of a computational approach vis-à-vis an experimental one in designing DHA/VHF MOST systems. The present work is an attempt to fill this gap.

Specifically, we here introduce an easily calculable descriptor for assessing the overall potency of any MOST system by combining three separate performance criteria, and then use DFT methods to obtain the values of this descriptor for 52 newly designed DHA/VHF compounds. While this represents a thorough bottom-up approach to the design of new MOST systems, two other unique facets of this endeavor relative to previous research should also be pointed out. First, while two of the criteria considered pertain to the values of $\Delta G_{storage}$ and $\Delta G^{\ddagger}$, the third involves the spectral mismatch between the parent and photoproduct isomers, which (as noted above) is seldom taken into account when an optimal MOST system is constructed, although its importance is well recognized. Second, the introduction and use of an all-around descriptor to quantify the overall MOST potential facilitate the design of compounds that simultaneously fulfill several of the relevant key requirements, which is one of the major challenges in this field of research.[2,5,51] For some of the DHA/VHF compounds that emerge as particularly promising from the screening, we

© 2023 The Authors. Published by Wiley-VCH GmbH

26289725, 0, Downloaded from https://chemistry-europe.onlinelibrary.wiley.com/doi/10.1002/cmtd.202200060 by Linkoping Universitet, Wiley Online Library on [03/04/2023]. See the Terms and Conditions (https://onlinelibrary.wiley.com/terms-and-conditions) on Wiley Online Library for rules of use; OA articles are governed by the applicable Creative Commons License

also investigate whether the DHA→VHF photoconversion is a facile reaction, as required for efficient MOST applications, and explore ways to improve their solubility in polar solvents like water, which is another major obstacle when devising MOST systems based on organic molecules. Furthermore, we propose different ways to synthesize the DHA/VHF compounds in question from commercially available reagents.

Computational Methods

Using the Gaussian 16 software,[52] geometry optimizations, harmonic frequency calculations and intrinsic reaction coordinate (IRC) calculations[53] in the S_0 state were carried out with the M06-2X density functional[54] in combination with the cc-pVDZ basis set.[55] Potential-energy minima and transition structures (TSs) were characterized as stationary points having only real vibrational frequencies or one imaginary vibrational frequency along the relevant normal mode, respectively. Based on the calculated frequencies, Gibbs free energies at room temperature were derived within the standard ideal-gas and rigid-rotor approximations. Furthermore, based on the resulting geometries, more accurate electronic energies were obtained by performing single-point calculations at the M06-2X/cc-pVTZ level of theory.

For the S_1 state, all calculations (geometries, frequencies and IRC) were done in the framework of time-dependent DFT (TD-DFT)[56] at the same levels that were employed for the S_0 state. Moreover, using the SHARC 2.0 package[57,58] interfaced with ORCA 4.2.1[59] and Gaussian 16, minimum-energy S_1/S_0 conical intersections (CIs) were located at the TD–M06-2X/cc-pVDZ level. Unless otherwise indicated, all calculations were performed in the gas phase, because the ideal solvents for the 52 neutral DHA/VHF compounds considered are non-polar, organic ones.[28,35,43,44] In complementary calculations in which three additional compounds derivatized for use in polar solvents were investigated, the SMD approach[60] was employed to model a water solvent.

UV-vis absorption spectra were calculated from vertical excitation energies (at S_0 molecular geometries) and oscillator strengths obtained at the TD-M06-2X/cc-pVTZ level. A sufficient number of excited states were included in the calculations to describe the full near-UV/visible range. The spectra were derived through convolution with Gaussian functions, each of them centered at a given excitation energy, with a height equal to the corresponding oscillator strength and a half-width of 0.3 eV. A motivation for this specific choice of half-width is given in Section 1.1 in the Supporting Information.

Results and Discussion

Parameter for spectral mismatch and all-around performance descriptor

In order to include the spectral mismatch between the parent and photoproduct isomers among the MOST performance criteria, one needs to define a parameter for measuring this mismatch in a relevant and quantitative way. For example, the difference in wavelengths of maximum UV-vis absorption of the two isomers is not a very useful parameter, as it only provides a relevant measure when the corresponding spectra consist of single and relatively sharp peaks with identical or near-identical widths. Another tentative parameter is the root mean square deviation between the spectra; however, as it has no upper bound, the values of this parameter are not transferable between MOST systems of different chemical types. With these reservations, the dimensionless parameter that we are proposing is the product of the normalized absorption spectra of the two isomers (denoted 1 and 2), integrated over the full near-UV/visible regime (300–800 nm). Specifically, denoting this parameter as the spectral overlap integral S [Equation (1)]:

$$S_{12} = \int_{300}^{800} nA_1(\lambda)A_2(\lambda)\mathrm{d}\lambda, \tag{1}$$

where n (with unit length^{-1}) is the product of the normalization constants for A_1 and A_2, determined in such a way that $S_{11} = S_{22} = 1$. With this definition, the goal to maximize the spectral mismatch is equivalent to minimize the value of S. Since this parameter can only take on values between 0 (maximal mismatch) and 1 (no mismatch), it can be used to compare any two MOST systems in a meaningful way. Furthermore, as illustrated in Figure 2, it can also be applied when the spectra in question have different numbers of peaks and the peaks have different widths.

Noting that $\Delta G_{\mathrm{storage}}$ and $\Delta G^{\ddagger}$ values of 0.30 MJ kg^{-1} and 100 kJ mol^{-1}, respectively, have been put forth as suitable thresholds towards which the design of MOST systems should be aimed,[2,6] it is natural to define an analogous threshold value for S. Here, following an analysis that is presented in Section 1.2 in the Supporting Information and is intended to make this

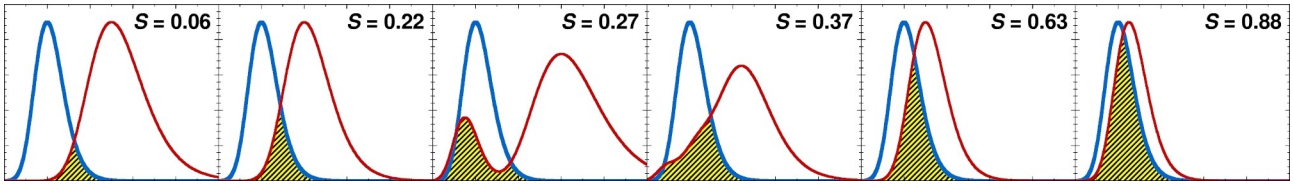

Figure 2. Calculated S values for the spectral mismatch between the parent and photoproduct isomers for model spectra of different qualitative types. The overlap region is highlighted in yellow-black font.

© 2023 The Authors. Published by Wiley-VCH GmbH

definition less arbitrary, we suggest that the threshold is set to 0.40. In a situation when the spectra of the two isomers consist of single peaks in the near-UV/visible range, this value corresponds to a difference in the wavelengths of maximum absorption of about 75 nm.

Given that an ideal MOST system maximizes $\Delta G_{storage}$ and $\Delta G^{\ddagger}$ and minimizes S, it is then natural to use these three parameters to define an all-around descriptor of the overall MOST potential as [Equation (2)]:

$$\mathrm{MAD} = \frac{4}{3}\frac{\Delta G^{\ddagger}\Delta G_{storage}}{S}, \quad (2)$$

where MAD is an acronym for MOST All-around Descriptor. Here, the 4/3 factor is introduced in order for a system that precisely meets each of the three separate thresholds ($\Delta G_{storage} \geq 0.30$ MJ kg^{-1}, $\Delta G^{\ddagger} \geq 100$ kJ mol^{-1}, $S \leq 0.40$) to have a MAD value of exactly 100 in the corresponding units (GJ^2 kg^{-1} mol^{-1}). Henceforth, these units are omitted but implied whenever MAD values are discussed. With this definition, it is one of the goals of the present work to identify DHA/VHF compounds whose MAD values are at least 100 and to understand chemically how such values can be attained.

Concerning the definition of the MAD index and its use, two comments are needed. The first is that the MAD index is intended to be an easily calculable descriptor, which is why it only includes parameters ($\Delta G_{storage}$, $\Delta G^{\ddagger}$ and S) whose values can be obtained by black-box DFT modelling. Thus, a few other parameters known to influence the efficiency of a MOST system, such as photoisomerization efficiency, photostability and solubility, are deliberately excluded, simply because the modelling required to reliably estimate their values (e.g., non-adiabatic molecular dynamics simulations) is much too expensive to be used in screening of many different DHA/VHF compounds. In this work, these aspects are instead addressed in a separate step *after* the MAD-based screening. The second comment is that calculated MAD values are not at all meant to be used in such a way that a compound showing a larger value than another compound is considered a "better" or more suitable MOST system by this virtue alone. Indeed, owing to a particularly good performance with respect to one or two of the $\Delta G_{storage}$, $\Delta G^{\ddagger}$ and S thresholds, it is of course possible for a compound that does not meet each of these thresholds to achieve a larger MAD value than a compound that does. Rather, the purpose of the MAD index is to help identify compounds with overall properties suitable for future MOST applications, as well as to facilitate further chemical tailoring by excluding underwhelming compounds from the candidate pool.

Screening of DHA/VHF compounds

Before describing and presenting the results of the screening of different DHA/VHF compounds for their all-around MOST potential, it is important to ascertain that the M06-2X-based calculations performed in this work provide reliable predictions of $\Delta G_{storage}$, $\Delta G^{\ddagger}$ and S. To this end, and as further discussed below, such calculations were performed to obtain $\Delta G_{storage}$ and $\Delta G^{\ddagger}$ values for three previously characterized DHA/VHF MOST systems in the literature (here denoted **E1**,[48] **E2**[38] and **E3**[39]). Moreover, as detailed in Section 2.1 in the Supporting Information, for one DHA/VHF compound it was demonstrated that the S value computed with the M06-2X density functional is quantitatively very similar to the S values obtained with two alternative density functionals: CAM-B3LYP[61] and wB97X-D.[62] In all calculations, the existence of different isomeric forms (of DHA, VHF and the TS for the thermal back-reaction) was accounted for by Boltzmann-averaging the values of $\Delta G_{storage}$, $\Delta G^{\ddagger}$ and S over the relevant isomers (for DHA, two isomers are possible if the C_1 position is heterosubstituted; for VHF, up to four isomers are possible upon C_1 heterosubstitution and C_2—C_3 rotation; for the TS, the back-reaction can occur through a conrotatory or a disrotatory mechanism.

Figure 3 presents the comparison of the previously reported $\Delta G_{storage}$ and $\Delta G^{\ddagger}$ values for compounds **E1**–**E3**[38,39,48] with the values calculated in this work. Pleasingly, the agreement between the two sets of data is generally very good, which lends credence to our computational methodology. Additionally, we also calculated the S and MAD values for **E1**–**E3**, whereby **E3** was found to achieve the largest MAD value by an appreciable margin (159 vs. 50 for **E2**). This finding corroborates that **E3** is among the best DHA/VHF MOST systems available today.[39] However, its large MAD value is partly a result of overcompensation. Indeed, while its $\Delta G^{\ddagger}$ value of 84 kJ mol^{-1} lies firmly below the 100 kJ mol^{-1} threshold, this deficiency is well compensated for by its excellent $\Delta G_{storage}$ and S values of 0.47 MJ kg^{-1} and 0.33, respectively.

Starting from the DHA/VHF core structure, the 52 compounds subjected to the screening were generated by varying the C_1 substituents and considering two different aryl groups at C_2, both in the absence of a secondary connection between C_3

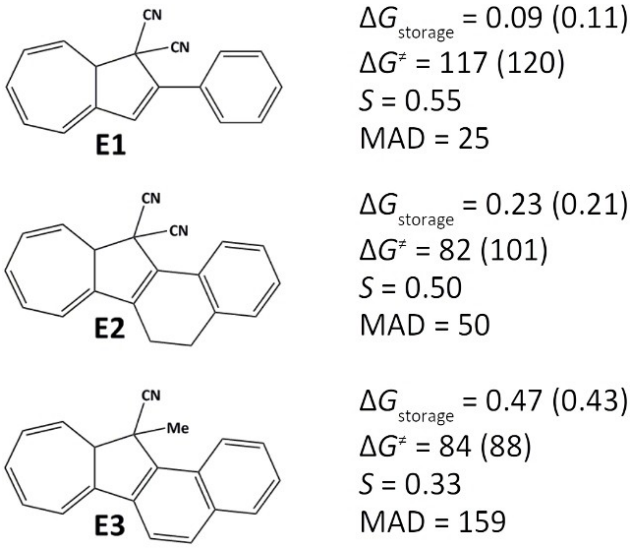

Figure 3. Structures of three previously developed DHA/VHF MOST systems and their $\Delta G_{storage}$ (in MJ kg^{-1}), $\Delta G^{\ddagger}$ (in kJ mol^{-1}), S and MAD values calculated in this work. The corresponding values reported in the original studies[38,39,48] are given in parentheses.

© 2023 The Authors. Published by Wiley-VCH GmbH

26289725, 0, Downloaded from https://chemistry-europe.onlinelibrary.wiley.com/doi/10.1002/cmtd.202200060 by Linkoping Universitet, Wiley Online Library on [03/04/2023]. See the Terms and Conditions (https://onlinelibrary.wiley.com/terms-and-conditions) on Wiley Online Library for rules of use; OA articles are governed by the applicable Creative Commons License

and the aryl, and in the presence of three different such connections. Regarding the C_1 substituents, it has been highlighted elsewhere that an electron-withdrawing group is needed for the thermal back-reaction to take place.[31,32] Therefore, in addition to already proposed monocyano and dicyano substitution patterns,[29,30,33] we also explored monosubstitution with a carboxylic acid, a 2-pyridyl sulfonyl (SO_2Py) group, a methyl ester, and a trifluoromethyl group, as well as disubstitution with SO_2Py and a methyl group. All of these substitutions were introduced with a specific goal in mind. The carboxylic acid should provide higher water solubility. The SO_2Py group, commonly used as a directing group in transition-metal catalysis,[63–67] might facilitate the Cu(1)-catalyzed back-reaction[43,44] by bringing the Cu^+ center closer to the C_1–C_2 bond. However, its strong electron-withdrawing capacity could also lower the $\Delta G^{\ddagger}$ value, which is why disubstitution with SO_2Py alongside an electron-donating methyl group was investigated as well. For a similar reason, it was also deemed natural to consider the comparatively weaker methyl ester and trifluoromethyl electron-withdrawing groups (the former by a mesomeric effect and the latter by an inductive effect).

For the C_2 aryl group, in turn, either a phenyl or a 2-pyridyl was used for their ability to act as a directing group in the Cu(1)-catalyzed back-reaction. Finally, regarding the secondary connection between C_3 and the aryl, we tested ethylenediyl (–CH_2CH_2–), methylene (–CH_2–) and –NH– (which provides some π-conjugation), as well as having no connector at all (to allow for C_2–C_3 rotations in the VHF isomer). Altogether, the combination of these four possibilities with the seven C_1 substituents and the two C_2 aryl groups yields 56 different DHA/VHF compounds. Out of these, only four have been previously described.[30,33,38] The remaining 52 ones subjected to the screening are shown in Figure 4.

The key results (calculated $\Delta G_{storage}$, $\Delta G^{\ddagger}$, S and MAD values) underlying the screening are summarized in Table 1, which also includes a quantity – the energy storage efficiency (ESE) – obtained by dividing $\Delta G_{storage}$ with the energy of maximum absorption of the DHA isomer. This quantity corresponds to the percentage of solar energy that is transformed to and stored as chemical energy in the VHF isomer. A number of observations can be made from Table 1. For example, provided that 40 compounds (77%) have a $\Delta G^{\ddagger}$ that exceeds 100 kJ mol^{-1}, it appears straightforward to find a DHA/VHF MOST system that can store the absorbed solar energy for a long time. Achieving a large $\Delta G_{storage}$, on the other hand, is more difficult, as only 21 compounds (40%) reach the 0.30 MJ kg^{-1} threshold. Notably, among those compounds, the average ESE value is 28%, which is quite comparable to that of 34% achieved by photosynthesis.[68] Notwithstanding, from the statistics it seems that an even greater challenge facing the design of a DHA/VHF MOST system is realizing sufficient spectral mismatch between DHA and VHF. In fact, only five compounds (10%) show an S value below the desired 0.40 limit, whereas as many as 22 compounds (42%) have an S value of 0.90 more. This challenge is likely to reflect that the size of the π-system and the conjugation length are relatively similar in the two isomers, which contrasts with the situation for other MOST systems (like norbornadienes and 1,2-azaborines) whose π-systems are more distinctly altered upon photoisomerization.

In the first step of the screening of the 52 DHA/VHF systems, only those compounds whose $\Delta G_{storage}$, $\Delta G^{\ddagger}$ and S values fulfill the conditions for Pareto optimality[69] were retained. Accordingly, any given compound with a specific set of $\Delta G_{storage}$, $\Delta G^{\ddagger}$

Table 1. Calculated $\Delta G_{storage}$ (in MJ kg^{-1}), ESE, $\Delta G^{\ddagger}$ (in kJ mol^{-1}), S and MAD values for the 52 DHA/VHF compounds studied in this work (Pareto-optimal compounds are underlined if their MAD values are smaller than 100, and are underlined and italicized if their MAD values are at least 100).

Compound	$\Delta G_{storage}$ (ESE)	$\Delta G^{\ddagger}$	S	MAD	Compound	$\Delta G_{storage}$ (ESE)	$\Delta G^{\ddagger}$	S	MAD
1	0.28 (21%)	122	0.97	47	**27**	0.31 (23%)	119	0.97	51
2	0.25 (26%)	115	0.78	49	**28**	0.26 (26%)	113	0.71	55
3	0.17 (18%)	113	0.97	26	**29**	0.20 (22%)	115	0.92	33
4	0.28 (22%)	120	0.98	46	**30**	0.30 (24%)	122	0.99	49
5	0.30 (24%)	128	0.95	54	**31**	0.30 (24%)	129	0.98	53
6	0.34 (28%)	108	0.97	50	**32**	0.22 (18%)	100	0.48	61
7	0.30 (32%)	91	0.82	44	**33**	0.34 (26%)	116	1.00	52
8	0.23 (28%)	98	0.70	43	**34**	0.36 (30%)	107	0.99	52
9	0.32 (28%)	111	0.97	49	**35**	0.33 (37%)	81	0.98	36
10	0.36 (32%)	113	0.78	69	**36**	0.25 (29%)	100	0.80	42
11	0.06 (5%)	111	0.43	21	**37**	0.34 (30%)	110	0.99	50
12	0.16 (11%)	130	0.92	30	**38**	0.38 (34%)	107	0.91	60
13	0.26 (20%)	112	0.84	46	**39**	0.08 (6%)	112	0.34	35
14	0.23 (25%)	102	0.99	32	**40**	0.16 (11%)	135	0.58	50
15	0.24 (28%)	94	0.92	33	**41**	0.23 (18%)	123	0.91	41
16	0.24 (19%)	117	0.84	44	**42**	0.21 (23%)	100	0.60	47
17	0.28 (24%)	120	0.99	45	**43**	0.22 (25%)	87	0.76	33
18	0.15 (11%)	89	0.58	31	**44**	0.22 (18%)	121	0.77	46
19	*0.24 (17%)*	*119*	*0.33*	*115*	**45**	0.38 (24%)	107	0.91	60
20	*0.34 (26%)*	*98*	*0.31*	*144*	**46**	0.18 (14%)	87	0.57	37
21	0.29 (31%)	88	0.33	103	**47**	0.26 (18%)	118	0.47	87
22	0.30 (33%)	79	0.48	66	**48**	0.29 (22%)	119	0.48	96
23	*0.33 (26%)*	*100*	*0.30*	*147*	**49**	0.30 (31%)	81	0.44	74
24	*0.35 (29%)*	*113*	*0.36*	*146*	**50**	0.29 (32%)	75	0.42	69
25	0.14 (10%)	120	0.57	39	**51**	0.31 (25%)	106	0.43	102
26	0.24 (17%)	137	0.90	49	***52***	*0.37 (30%)*	*112*	*0.46*	*120*

© 2023 The Authors. Published by Wiley-VCH GmbH

26289725, 0, Downloaded from https://chemistry-europe.onlinelibrary.wiley.com/doi/10.1002/cmtd.202200060 by Linkoping Universitet, Wiley Online Library on [03/04/2023]. See the Terms and Conditions (https://onlinelibrary.wiley.com/terms-and-conditions) on Wiley Online Library for rules of use; OA articles are governed by the applicable Creative Commons License

Research Article
doi.org/10.1002/cmtd.202200060
Chemistry Europe
European Chemical Societies Publishing

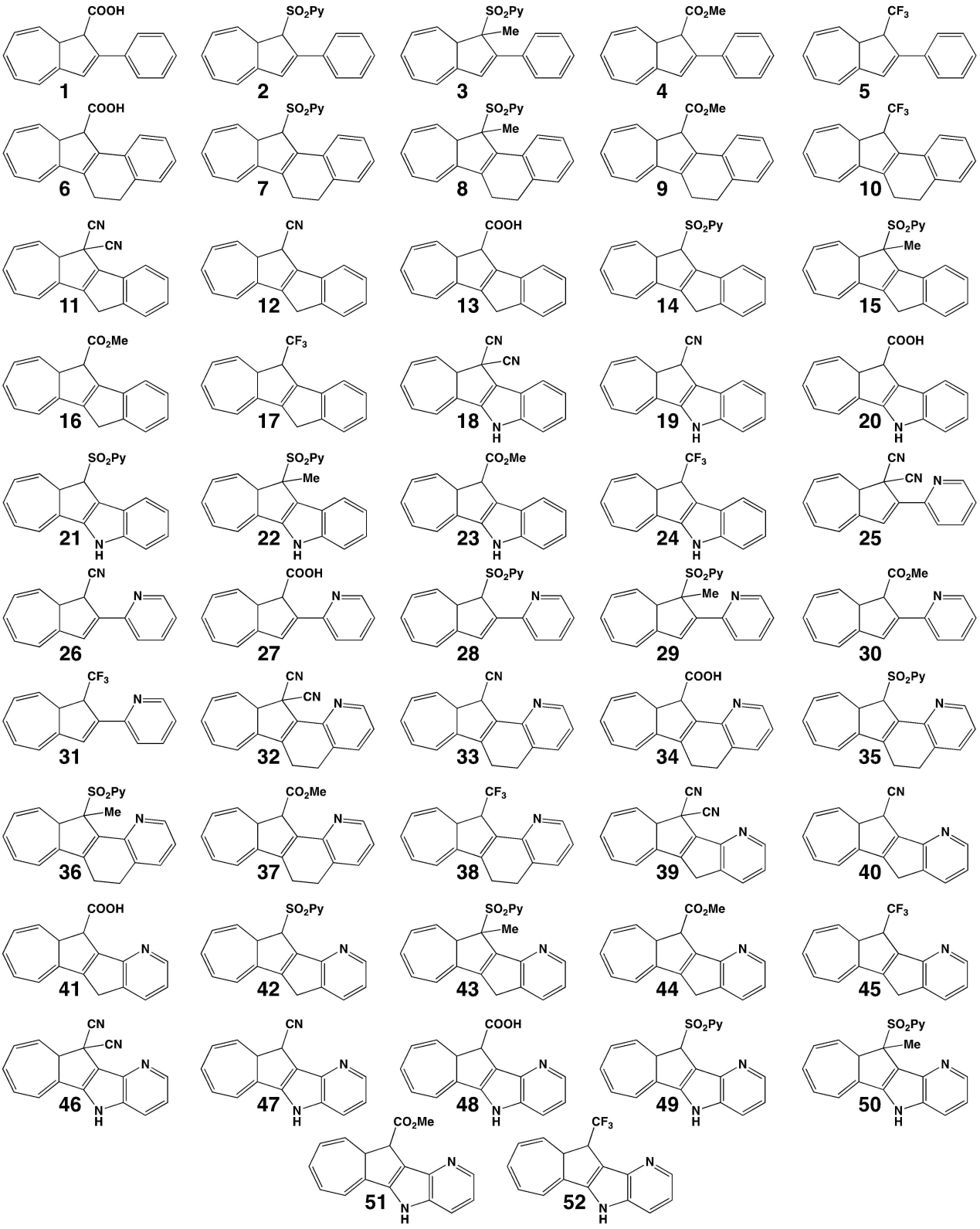

Figure 4. The 52 DHA/VHF compounds whose MOST potential was tested in this work.

and *S* values is Pareto-optimal only if there is no other compound that improves one (or more) of these values *without* worsening the other ones. Through this step, the number of compounds subsequently subjected to the MAD-based screening is reduced from 52 to 18 on simple numerical grounds, regardless of their MAD values. The 18 retained compounds are

© 2023 The Authors. Published by Wiley-VCH GmbH

26289725, 0, Downloaded from https://chemistry-europe.onlinelibrary.wiley.com/doi/10.1002/cmtd.202200060 by Linkoping Universitet, Wiley Online Library on [03/04/2023]. See the Terms and Conditions (https://onlinelibrary.wiley.com/terms-and-conditions) on Wiley Online Library for rules of use; OA articles are governed by the applicable Creative Commons License

Research Article
doi.org/10.1002/cmtd.202200060
Chemistry Europe
European Chemical Societies Publishing

underlined in Table 1. In the second step, **19**, **20**, **23**, **24** and **52** were identified as the subset of these compounds having a MAD value of at least 100 (underlined and italicized in Table 1), meaning that they either (**23** and **24**) meet all separate thresholds ($\Delta G_{storage} \geq 0.30$ MJ kg^{-1}, $\Delta G^{\ddagger} \geq 100$ kJ mol^{-1}, $S \leq 0.40$), or (**19**, **20** and **52**) compensate the non-fulfilment of a threshold by sufficiently exceeding another. Interestingly, these five compounds, among which **20**, **23** and **24** are the stand-out performers with MAD values of 144–147, are structurally very similar. Specifically, the only variation among **19**, **20**, **23** and **24** is the C_1 substituent, and **52** is the 2-pyridyl variant of **24**. Moreover, the common structural denominator for the five compounds is their NH connector between C_3 and the aryl group. Notably, this motif is present also in two other compounds, **21** and **51**, that attain a MAD value of at least 100 but are not Pareto-optimal.

The success of the NH connector is a result of an intricate interplay between several different factors, and can be better understood if one compares the corresponding molecules with their methylenic counterparts (for instance, comparing **23** with **16**), which have nearly identical molecular masses and geometries. In 2016, Mikkelsen and coworkers showed that the incorporation of a primary amino group at C_3 helps increase $\Delta G_{storage}$.[48] In the present case, the NH connector functions as a secondary amine and although its electron-donating capacity is weaker due to the conjugation of its lone pair with the C_2 aryl group, it is sufficiently strong to provide a boost in $\Delta G_{storage}$ (from 0.24 MJ kg^{-1} in **16** to 0.33 MJ kg^{-1} in **23**). However, this comes at the cost of a decrease in $\Delta G^{\ddagger}$ (from 117 kJ mol^{-1} in **16** to 100 kJ mol^{-1} in **23**). Still, this decrease is not severe and is not incompatible with long energy-storage times. Despite these effects, the main advantage of the NH connector is its ability to drastically increase the spectral mismatch, with the *S* value of 0.84 for **16** being reduced to a markedly better 0.30 for **23**. Notably, as further detailed in Section 2.2 in the Supporting Information, while the additional conjugation in **23** shifts the absorption of the DHA isomer only marginally (from 354 nm in **16** to 346 nm in **23**), it does cause a pronounced red-shift in the absorption of the VHF isomer (from 376 nm in **16** to 440 nm in **23**), which explains the improved *S* value. All in all, these results provide strong support for the conclusion that a NH connector between C_3 and an aryl group at C_2 is a key structural element for constructing potent MOST systems based on the DHA/VHF core.

Having completed the screening, the subsequent parts of this work will explore the extent to which some of the compounds with the highest MAD scores exhibit other desirable MOST features. For this, we will primarily focus on **23** and, to a lesser extent, on **20** (which is structurally very similar to **23** and whose $\Delta G_{storage}$, $\Delta G^{\ddagger}$, *S* scores are almost identical to those of **23**). The first feature of interest is ease of synthesis.

Retrosynthetic analysis of compound 23

Compounds **20** and **23** contain two structural elements that are not present in any of the DHA/VHF systems synthesized to date: the NH connector and a single carboxylate derivative substituent at C_1. At first glance, the ester **23** could be obtained by esterification of **20**, which, in turn, may be produced from a dicyano parent compound through reduction to the monocyano species with DIBAL-H[33] and subsequent hydrolysis. The NH connector, on the other hand, is a different prospect. In 2016, Nielsen and coworkers synthesized a DHA/VHF system bearing an unsaturated connector (–CHCH–),[39] but this moiety was not present on the starting material. Rather, it was generated at the last step of the synthesis from the saturated precursor. Therefore, it is necessary to define an alternative approach to the synthesis of **20** or **23** that incorporates the NH connector. Figure 5 presents a possible retrosynthetic sequence, decomposing **23** into simple, commercially available reagents.

In 2008, Maes and coworkers described the synthesis of indole derivatives via tandem palladium-catalyzed C–N/C–C cross coupling between 4-chloroquinolines and 2-chloroanilines.[70] The reaction involves an initial Buchwald-Hartwig amination immediately followed by intramolecular cyclization, forming exclusively a 5-membered ring. This process would allow the installation of both the phenyl group and the NH connector in a single step, from 2-chloroaniline and the ketone intermediate **I2**, activated as a vinyl triflate. The cyclopentanone of this intermediate could come from an intramolecular Heck reaction, forming the C_3–C_{3a} bond. This process requires activating the carboxylic acid, for instance as an acyl chloride; a similar process has been described using anhydrides.[71] To ensure that the correct carboxylate is activated, the methyl ester has to be formed prior to this step to act as a protecting group.

Intermediate **I1** in Figure 5 is formally a succinic acid derivative, but a sequence of alkylation of the succinic

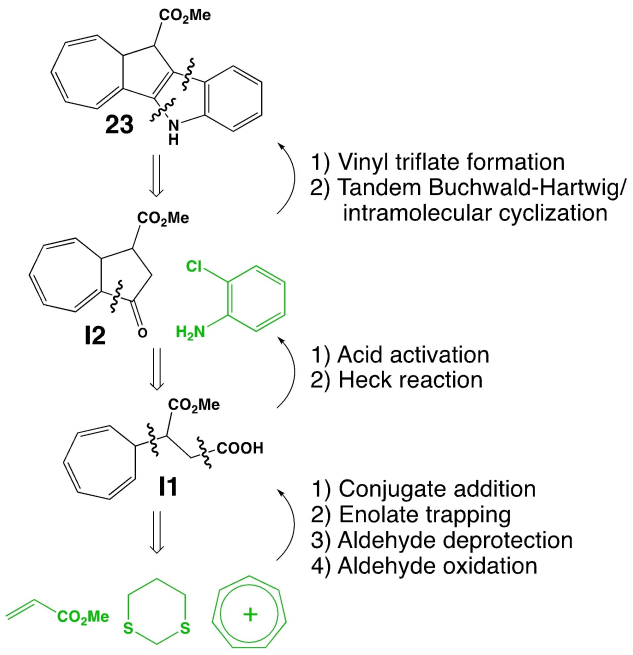

Figure 5. Retrosynthetic analysis of compound **23** and the reactions involved in each step. Molecules drawn in green font are commercially available.

© 2023 The Authors. Published by Wiley-VCH GmbH

26289725, 0, Downloaded from https://chemistry-europe.onlinelibrary.wiley.com/doi/10.1002/cmtd.202200060 by Linkoping Universitet, Wiley Online Library on [03/04/2023]. See the Terms and Conditions (https://onlinelibrary.wiley.com/terms-and-conditions) on Wiley Online Library for rules of use; OA articles are governed by the applicable Creative Commons License

Research Article
doi.org/10.1002/cmtd.202200060
Chemistry Europe
European Chemical Societies Publishing

anhydride enolate and transesterification with methanol would afford little control over the final position of the tropylium relative to the methyl ester, as the methyl ester can be formed at any of the positions. Better regiocontrol is realized if the carboxylic acid is incorporated to methyl acrylate in the form of a nucleophilic reagent, and the enolate intermediate is captured with a tropylium salt (i.e., tetrafluoroborate). In this way, deprotonation of 1,3-dithiane with BuLi/CuI would generate the lithium dialkylcuprate, which undergoes 1,4-addition to methyl acrylate; the resulting enolate is trapped by the tropylium cation to afford α-alkylation. Removal of the thioacetal protecting group and oxidation of the resulting aldehyde would finally yield **I1**.

This seven-step process (conjugate addition→enolate trapping→aldehyde deprotection→aldehyde oxidation→acid activation→intramolecular Heck→triflate formation→C–N/C–C cross coupling) for the preparation of **23**, with only one additional hydrolysis step required for its conversion to **20**, indicates that both compounds are synthetically feasible. Further support for this notion is provided in Section 3 in the Supporting Information, which includes a more detailed synthetic sequence based on the analysis in Figure 5 (see Figure S6 in the Supporting Information) and also an alternative sequence starting instead from 3-oxindole (see Figure S7 in the Supporting Information).

While other synthetic routes to the preparation of **23** are likely possible, the two routes put forth herein serve to show that installation of the NH connector is feasible, either in the final step (route in Figure S6) or by providing this motif already from the beginning (route in Figure S7). In terms of number of steps, these two routes are comparable, involving seven steps (Figure S6) or six steps plus the steps needed to prepare 3-oxindole (Figure S7). As such, the routes are also comparable to those used to prepare the aforementioned **E2**[38] and **E3**[39] compounds, both of which required six steps plus preparation of the starting material.

Derivatization of compounds 20 and 23 for better solubility in polar solvents

Another desirable feature of MOST systems is that they are soluble in polar solvents like water. However, for the majority of MOST systems hitherto developed based on organic molecules, this is a major hurdle and non-polar, organic solvents are required.[28,35,43,44] In this light, the reason for including a carboxylic acid among the C_1 substituents considered in the screening is precisely its naturally high solubility in water. Accordingly, we expect compound **20** to be at least partially soluble in water, especially in its deprotonated state (**20 A**) at neutral pH. Compound **23**, on the other hand, does not contain any functional group that enhances water solubility. However, whereas it is well known that the addition of almost any functional group to the DHA/VHF core can lead to drastic changes in the chemical properties,[34–37,48] one key advantage of **23** is that it can be derivatized with minimal effect on the DHA/VHF core by replacing the methyl group of its methyl ester by another substituent. In this way, it might be possible to improve the water solubility without altering the $\Delta G_{storage}$, $\Delta G^{\ddagger}$ and S values too much.

However, in order to maintain $\Delta G_{storage}$ above the 0.30 MJ kg^{-1} threshold, there is clearly a limit on how large this substituent can be. Noting that the $\Delta G_{storage}$ of 0.33 MJ kg^{-1} attained by **23** comes from a DHA/VHF free-energy difference of ~91 kJ mol^{-1} and a molecular mass of ~277 g mol^{-1}, it might be possible to increase the latter value to ~304 g mol^{-1} without going below the 0.30 MJ kg^{-1} threshold (assuming that the free-energy difference is relatively independent on the choice of substituent). Although this margin is quite small, it is sufficient for replacing the methyl group of **23** with ethanolamine (yielding compound **23 A** in a protonated state at neutral pH) or ethylene glycol (yielding compound **23 B**), whose NH_3^+/OH groups should increase water solubility. With these changes introduced, it is of interest to compare how well **20 A**, **23 A** and **23 B** perform compared to the parent compounds. Therefore, their $\Delta G_{storage}$, $\Delta G^{\ddagger}$ and S and MAD values were calculated in the same way as before, but this time accounting for the presence of a water solvent with the use of the SMD approach.[60] The results are given in Figure 6.

Encouragingly, the results for **20 A** are very similar to the previous results for **20** (see Table 1). **23 A** and **23 B**, on the other hand, perform much worse than **23** (see Table 1). This is due primarily to an increase in the S value and a decrease in $\Delta G^{\ddagger}$, the latter of which may reflect zwitterionic character in the TS[72] and an ensuing stabilization by the water solvent. As shown in Section 2.3 in the Supporting Information, the increase in the S value arises from the absorption of the DHA and VHF isomers in water being brought into the same region through a pronounced red-shift in the absorption of the latter species.

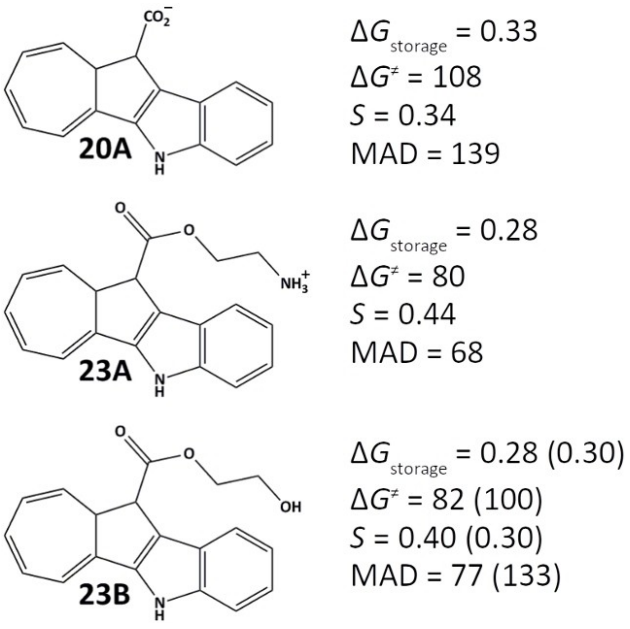

Figure 6. Structures of derivatized compounds **20 A**, **23 A** and **23 B** and their calculated $\Delta G_{storage}$ (in MJ kg^{-1}), $\Delta G^{\ddagger}$ (in kJ mol^{-1}), S and MAD values. For **23 B**, values in parentheses are the corresponding ones calculated in the gas phase.

© 2023 The Authors. Published by Wiley-VCH GmbH

26289725, 0, Downloaded from https://chemistry-europe.onlinelibrary.wiley.com/doi/10.1002/cmtd.202200060 by Linkoping Universitet, Wiley Online Library on [03/04/2023]. See the Terms and Conditions (https://onlinelibrary.wiley.com/terms-and-conditions) on Wiley Online Library for rules of use; OA articles are governed by the applicable Creative Commons License

Research Article
doi.org/10.1002/cmtd.202200060
Chemistry Europe
European Chemical Societies Publishing

Taken together, the results in Figure 6 suggest that **20** (in the form of **20 A**) could well be a suitable MOST system for use in a polar solvent and, in the case of **23**, that using a non-polar, organic solvent is preferable over derivatization towards a polar solvent. Importantly, however, the worse performance of **23 A** and **23 B** relative to **23** is not an intrinsic consequence of their ethanolamine (**23 A**) and ethylene glycol (**23B**) substituents, but is rather due to the polar water environment. Indeed, this is clear from the observation in Figure 6 that the $\Delta G_{storage}$, $\Delta G^{\ddagger}$ and S and MAD values for **23 B** calculated in the gas phase agree very well with the corresponding results for **23** (see Table 1). Furthermore, from complementary calculations summarized in Section 4.1 in the Supporting Information that compare the gas-phase values for **23 B** (MAD = 133) with those calculated in different solvents, it can be inferred that while this compound largely maintains its excellent MOST properties in a non-polar toluene solvent (MAD = 120), the properties deteriorate with increasing solvent polarity (MAD = 105/77 in acetonitrile/water), again primarily because of a decrease in $\Delta G^{\ddagger}$ and an increase in the S value.

Besides investigating how the MOST properties are influenced by increasing solvent polarity, it is also of interest to assess the actual water solubilities of some of the current DHA/VHF compounds, as high values would indicate that their heat release is efficient in this solvent. While it is clearly beyond the scope of this work to try to calculate absolute water solubilities, which is a significant undertaking in its own right,[73] solubilities in water relative to a non-polar solvent like *n*-octanol can be accurately predicted through DFT/SMD-based calculation of the water-octanol partition coefficient (P).[74] Usually expressed as a common logarithm (log$P$), this coefficient was calculated for compounds **23**, **23 A**, **23 B** and **20 A**, as well as for the previously characterized compounds **E1**–**E3**,[38,39,48] as described in Section 4.2 in the Supporting Information. The results, obtained by Boltzmann-averaging over the relevant DHA and VHF isomers, are summarized in Figure S9 in the Supporting Information. Noting that a predominantly hydrophilic/hydrophobic compound with better/worse solubility in water than in *n*-octanol is associated with a negative/positive log$P$ value, **23** is, as expected, predicted to be less soluble in water than in *n*-octanol (log$P$ = 0.72). Still, **23** exhibits better water solubility than each of **E1**–**E3** (which have log$P$ values of 0.75–1.02). Furthermore, the derivatization of **23** does indeed improve the water solubility, with **23 B** showing a reduced log$P$ value of 0.59 and **23 A** even attaining a pronounced negative log$P$ value of −0.36, most likely because of its cationic ammonium group. A negative log$P$ value is also achieved by the anionic **20 A**, which appears to be the most water soluble of the compounds considered (log$P$ = −0.82).

DHA→VHF photoconversion of compound 23

Despite the favorable steady-state properties of **20** and **23** documented herein, these compounds would not be particularly useful as MOST systems unless their DHA→VHF photoconversion processes are facile. Therefore, we decided to investigate this issue by mapping the relevant parts of the S_0 and S_1 potential energy surfaces (PESs) of **23** through TD-M06-2X calculations. Given the chemical similarity of **20** and **23**, the results for **23** are likely to be relevant also for **20**. Moreover, seeking to address the DHA→VHF photoconversion only, no other deactivation channels leading to the formation of undesirable side-products were considered. The results are presented in Figure 7 and some of the associated key structures are shown in Figure 8.

In the most stable DHA diastereoisomer of **23** (denoted **23**-DHA-1 in Figure 7), the H atom at C_{8a} and the CO_2Me group at

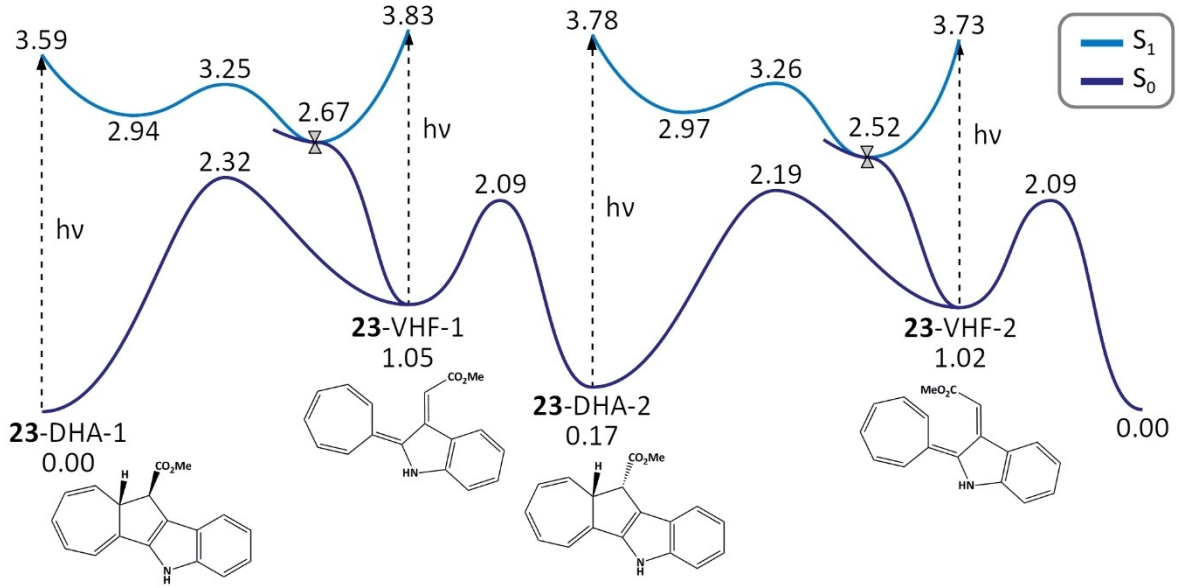

Figure 7. PESs describing the interconversion of DHA and VHF isomers of compound **23** in the S_0 and S_1 states. Electronic energies are given in eV relative to the S_0 energy of the most stable isomer (denoted **23**-DHA-1). CIs are indicated with hourglass symbols.

© 2023 The Authors. Published by Wiley-VCH GmbH

26289725, 0, Downloaded from https://chemistry-europe.onlinelibrary.wiley.com/doi/10.1002/cmtd.202200060 by Linkoping Universitet, Wiley Online Library on [03/04/2023]. See the Terms and Conditions (https://onlinelibrary.wiley.com/terms-and-conditions) on Wiley Online Library for rules of use; OA articles are governed by the applicable Creative Commons License

Research Article
doi.org/10.1002/cmtd.202200060
Chemistry Europe
European Chemical Societies Publishing

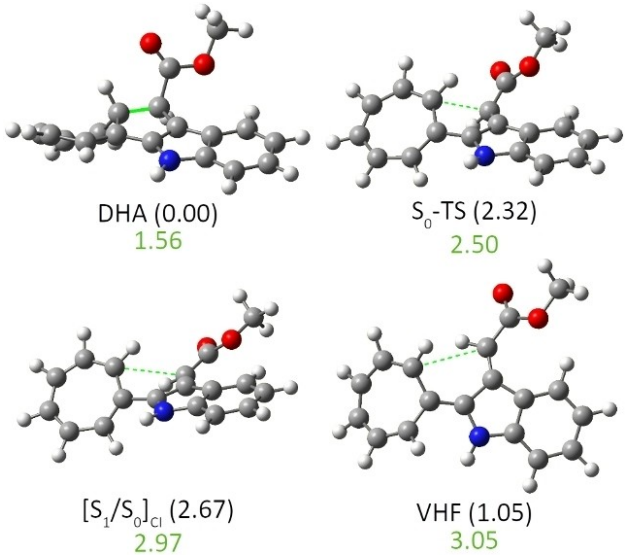

Figure 8. Key structures for the **23**-DHA-1→**23**-VHF-1 photoconversion. Relative electronic energies (in parentheses) are given in eV and C_1–C_{8a} distances (in green font) are given in Å. C, H, O and N atoms in grey, light-grey, red and blue font, respectively.

C_1 are *syn* oriented (see also Figure 8). Starting from this species, the corresponding Franck-Condon (FC) point in the S_1 state (with ππ* character) is populated by UV-A irradiation of 3.59 eV (345 nm). This point is connected to an S_1 minimum at 2.94 eV, at which the seven-membered ring adopts a planar geometry. Such intermediate planarization of the DHA core has also been observed in non-adiabatic molecular dynamics simulations of other DHA/VHF compounds.[46] From this minimum, which is further characterized in Section 5 in the Supporting Information, accessing the photoreactive CI with the S_0 state at 2.67 eV requires that an energy barrier of 0.31 eV is surmounted. Given that the associated TS lies 0.34 eV below the FC point, it seems likely that the photoexcited system is sufficiently energetic to overcome this barrier.

Regarding the photoreactive CI, it exhibits a number of features that point to the fact that it does funnel the system forward to the **23**-VHF-1 photoproduct diastereoisomer, rather than back to the starting **23**-DHA-1 diastereoisomer. First, with a C_1–C_{8a} distance of 2.97 Å (see Figure 8), it occurs "beyond" the TS (at 2.50 Å) between **23**-DHA-1 and **23**-VHF-1 along the S_0 PES, which means that while **23**-VHF-1 can be reached in a barrierless fashion, **23**-DHA-1 cannot. Second, as illustrated in Section 6 in the Supporting Information, neither the S_0 gradient nor the S_1-S_0 gradient difference vectors at the CI show any tendency of the system being funneled back to **23**-DHA-1. These very features further ensure that accessing this CI through light absorption by **23**-VHF-1, which is also possible (see Figure 7), is not detrimental to the energy storage. Rather, this improves the MOST functionality of the system by increasing its photostability. All in all, then, the mechanism for the DHA→VHF photoconversion that emerges from the calculations appears fully compatible with the use of **23** as a MOST system.

Starting from **23**-VHF-1, Figure 7 reveals that the kinetically favored product of the thermal back-reaction is not the initial DHA diastereoisomer, **23**-DHA-1 (barrier of 1.27 eV), but rather **23**-DHA-2 (1.04 eV), in which the H atom at C_{8a} and the CO_2Me group at C_1 are *anti* oriented. This is consistent with the well-known rule for electrocyclic reactions that a thermal process occurs by a disrotatory mechanism if the corresponding photochemical process proceeds by a conrotatory mechanism, and vice versa. However, since UV–A irradiation of **23**-DHA-2 subsequently and analogously produces the **23**-VHF-2 photoproduct diastereoisomer, the fact that the thermal back-reaction of this species similarly favors formation of **23**-DHA-1 (barrier of 1.07 eV) over **23**-DHA-2 (1.17 eV) means that a fully reversible photoswitching process is possible. This has a key implication for the design of a synthetic route towards **23** in that a diastereoselective sequence is not needed, as any given diastereosisomer will be transformed into the other as the photochemical-thermal reaction cycle is continuously operated.

A final remark

Having put forth and illustrated the use of the MAD index, it is important to reemphasize that this index should not be considered a tool for identifying the ideal MOST system, but rather as a tool that can simplify the identification of a few overall well-performing MOST systems from a much larger pool of candidate compounds. Specifically, this is achieved by eliminating from consideration a significant portion of compounds on numerical grounds alone, for example, their failure to fulfill the conditions for Pareto optimality *and* to reach a MAD value of at least 100. In the present case, starting from a pool of 52 molecules, this helped reduced the number of candidate compounds worthy of further chemical scrutiny by one order of magnitude, from 52 to 5. This reduction, we believe, attests to the usefulness of the MAD index.

Conclusions

In summary, we have presented a bottom-up study aimed at designing more efficient DHA/VHF MOST systems based on the results of extensive DFT calculations, with a particular goal to unveil specific DHA/VHF compounds that fulfill as many key MOST performance criteria as possible within one and the same molecular framework. This goal, which is of central importance to the field,[2,5,51] is addressed by combining three separate criteria into one easily calculable, overall MOST performance descriptor. Specifically, this descriptor, which we term MAD (MOST All-around Descriptor), incorporates not only the values of $\Delta G_{storage}$ and $\Delta G^{\ddagger}$, but also a property that rarely ever is taken into account when an optimal MOST system is designed. This property is the spectral mismatch between the DHA and VHF isomers, which we quantify using a parameter referred to as the spectral overlap integral *S*. In an ideal situation where the spectral mismatch is large, this parameter has a small value.

© 2023 The Authors. Published by Wiley-VCH GmbH

26289725, 0, Downloaded from https://chemistry-europe.onlinelibrary.wiley.com/doi/10.1002/cmtd.202200060 by Linkoping Universitet, Wiley Online Library on [03/04/2023]. See the Terms and Conditions (https://onlinelibrary.wiley.com/terms-and-conditions) on Wiley Online Library for rules of use; OA articles are governed by the applicable Creative Commons License

By calculating MAD values for 52 entirely novel DHA/VHF compounds using a level of theory that accurately reproduces the $\Delta G_{storage}$ and $\Delta G^{\ddagger}$ values shown by previously characterized compounds,[38,39,48] several key insights are gained for the future construction of MOST systems based on the DHA/VHF couple. First, it is found that achieving a distinct DHA/VHF spectral mismatch (i.e., a small *S* value) is much more challenging than reaching large $\Delta G_{storage}$ and $\Delta G^{\ddagger}$ values. Second, despite this challenge, our screening identifies two Pareto-optimal compounds (**23** and **24**) that simultaneously meet all separate thresholds invoked for the $\Delta G_{storage}$ ($\geq$0.30 MJ kg^{-1}), $\Delta G^{\ddagger}$ ($\geq$ 100 kJ mol^{-1}) and *S* ($\leq$ 0.40) values, thereby attaining MAD scores that exceed the target value of 100. Furthermore, the screening also picks out three Pareto-optimal compounds (**19**, **20** and **52**) that surpass this value by compensating the non-fulfilment of a threshold through the fulfilment of another. Notably, these five compounds share a common structural motif in the form of a NH connector between the C_3 position and an aryl group at the C_2 position. Accordingly, we propose that this motif, which is not included in any of the DHA/VHF compounds described in the existing literature,[33–36,38,39,75] is a key element for viable usage of such molecules as MOST systems.

Following the screening, the second part of the paper then explores the extent to which some of these five compounds (primarily **23** but also **20**) exhibit other desirable MOST features, including ease of synthesis, amenability to being derivatized for better solubility in polar solvents, and facile DHA→VHF photoconversion. To this end, we outline possible synthetic sequences for their preparation starting from either 1,3-dithiane or 3-oxindole, and present results for derivatized compounds showing that a likely water-soluble anionic form of **20** maintains its excellent MAD value in this solvent. For **23**, on the other hand, usage of a non-polar, organic solvent appears a better strategy than derivatization towards a polar solvent. Regarding the DHA→VHF photoconversion, in turn, calculated PESs and CIs for the S_0 and S_1 states show that this process is indeed facile for the compounds in question. Furthermore, this modelling predicts that the full DHA→VHF→DHA reaction cycle proceeds through interconversion of one diastereoisomeric form of DHA/VHF into the other. Hence, the synthesis of these compounds will not require a diastereoselective approach.

Altogether, we conclude that the use in this work of an original bottom-up computational approach has helped identify DHA/VHF compounds with excellent overall properties for future MOST applications.

Acknowledgements

This work was supported by the Olle Engkvist Foundation (grant 204-0183), the Swedish Research Council (grant 2019-03664), ÅForsk (grant 20-570) and the Carl Trygger Foundation (grant CTS 20:102). The calculations were enabled by resources provided by (a) the Swedish National Infrastructure for Computing at the National Supercomputer Centre partially funded by the Swedish Research Council (grant 2018-05973) and (b) the National Supercomputer Centre funded by Linköping University.

Conflict of Interest

The authors declare no conflict of interest.

Data Availability Statement

The data that support the findings of this study are available from the authors upon reasonable request.

Keywords: density functional calculations · electrocyclic reactions · energy conversion · photochemistry · photochromism

[1] T. J. Kucharski, Y. Tian, S. Akbulatov, R. Boulatov, *Energy Environ. Sci.* **2011**, *4*, 4449–4472.
[2] C.-L. Sun, C. Wang, R. Boulatov, *ChemPhotoChem* **2019**, *3*, 268–283.
[3] H. Wang, H. K. Bisoyi, X. Zhang, F. Hassan, Q. Li, *Chem. Eur. J.* **2022**, *28*, e202103906.
[4] A. Lennartson, A. Roffey, K. Moth-Poulsen, *Tetrahedron Lett.* **2015**, *56*, 1457–1465.
[5] Z. Wang, P. Erhart, T. Li, Z.-Y. Zhang, D. Sampedro, Z. Hu, H. A. Wegner, O. Brummel, J. Libuda, M. B. Nielsen, K. Moth-Poulsen, *Joule* **2021**, *5*, 3116–3136.
[6] V. A. Bren', A. D. Dubonosov, V. I. Minkin, V. A. Chernoivanov, *Russ. Chem. Rev.* **1991**, *60*, 451–469.
[7] S. J. Cristol, R. L. Snell, *J. Am. Chem. Soc.* **1958**, *80*, 1950–1952.
[8] Z.-I. Yoshida, *J. Photochem.* **1985**, *29*, 27–40.
[9] A. Dreos, K. Börjesson, Z. Wang, A. Roffey, Z. Norwood, D. Kushnir, K. Moth-Poulsen, *Energy Environ. Sci.* **2017**, *10*, 728–734.
[10] A. Dreos, Z. Wang, J. Udmark, A. Ström, P. Erhart, K. Börjesson, M. B. Nielsen, K. Moth-Poulsen, *Adv. Energy Mater.* **2018**, *8*, 1703401.
[11] M. Mansø, A. U. Petersen, Z. Wang, P. Erhart, M. B. Nielsen, K. Moth-Poulsen, *Nat. Commun.* **2018**, *9*, 1945.
[12] Z. Wang, A. Roffey, R. Losantos, A. Lennartson, M. Jevric, A. U. Petersen, M. Quant, A. Dreos, X. Wen, D. Sampedro, K. Börjesson, K. Moth-Poulsen, *Energy Environ. Sci.* **2019**, *12*, 187–193.
[13] M. Jevric, Z. Wang, A. U. Petersen, M. Mansø, C. J. Sumby, M. B. Nielsen, K. Moth-Poulsen, *Eur. J. Org. Chem.* **2019**, 2354–2361.
[14] J. Olmsted III, J. Lawrence, G. G. Yee, *Sol. Energy* **1983**, *30*, 271–274.
[15] A. M. Kolpak, J. C. Grossman, *Nano Lett.* **2011**, *11*, 3156–3162.
[16] A. E. Telgerafchi, M. Mehranpour, H. Nazockdast, *Chem. Phys. Lett.* **2018**, *707*, 113–116.
[17] W. Pang, J. Xue, H. Pang, *Sci. Rep.* **2019**, *9*, 5224.
[18] W. Moormann, T. Tellkamp, E. Stadler, F. Röhricht, C. Näther, R. Puttreddy, K. Rissanen, G. Gescheidt, R. Herges, *Angew. Chem. Int. Ed.* **2020**, *59*, 15081–15086; *Angew. Chem.* **2020**, *132*, 15193–15198.
[19] K. Morimitsu, K. Shibata, S. Kobatake, M. Irie, *J. Org. Chem.* **2002**, *67*, 4574–4578.
[20] J. C.-H. Chan, W. H. Lam, H.-L. Wong, N. Zhu, W.-T. Wong, V. W.-W. Yam, *J. Am. Chem. Soc.* **2011**, *133*, 12690–12705.
[21] N. M.-W. Wu, M. Ng, W. H. Lam, H.-L. Wong, V. W.-W. Yam, *J. Am. Chem. Soc.* **2017**, *139*, 15142–15150.
[22] B. Oruganti, P. P. Kalapos, V. Bhargav, G. London, B. Durbeej, *J. Am. Chem. Soc.* **2020**, *142*, 13941–13953.
[23] R. Boese, J. K. Cammack, A. J. Matzger, K. Pflug, W. B. Tolman, K. P. C. Vollhardt, T. W. Weidman, *J. Am. Chem. Soc.* **1997**, *119*, 6757–6773.
[24] M. R. Harpham, S. C. Nguyen, Z. Hou, J. C. Grossman, C. B. Harris, M. W. Mara, A. B. Stickrath, Y. Kanai, A. M. Kolpak, D. Lee, D.-J. Liu, J. P. Lomont, K. Moth-Poulsen, N. Vinokurov, L. X. Chen, K. P. C. Vollhardt, *Angew. Chem. Int. Ed.* **2012**, *51*, 7692–7696; *Angew. Chem.* **2012**, *124*, 7812–7816.

© 2023 The Authors. Published by Wiley-VCH GmbH

26289725, 0, Downloaded from https://chemistry-europe.onlinelibrary.wiley.com/doi/10.1002/cmtd.202200060 by Linkoping Universitet, Wiley Online Library on [03/04/2023]. See the Terms and Conditions (https://onlinelibrary.wiley.com/terms-and-conditions) on Wiley Online Library for rules of use; OA articles are governed by the applicable Creative Commons License

[25] K. Moth-Poulsen, D. Ćoso, K. Börjesson, N. Vinokurov, S. K. Meier, A. Majumdar, K. P. C. Vollhardt, R. A. Segalman, *Energy Environ. Sci.* **2012**, *5*, 8534–8537.
[26] K. Börjesson, D. Ćoso, V. Gray, J. C. Grossman, J. Guan, C. B. Harris, N. Hertkorn, Z. Hou, Y. Kanai, D. Lee, J. P. Lomont, A. Majumdar, S. K. Meier, K. Moth-Poulsen, R. L. Myrabo, S. C. Nguyen, R. A. Segalman, V. Srinivasan, W. B. Tolman, N. Vinokurov, K. P. C. Vollhardt, T. W. Weidman, *Chem. Eur. J.* **2014**, *20*, 15587–15604.
[27] K. Edel, X. Yang, J. S. A. Ishibashi, A. N. Lamm, C. Maichle-Mössmer, Z. X. Giustra, S.-Y. Liu, H. F. Bettinger, *Angew. Chem. Int. Ed.* **2018**, *57*, 5296–5300; *Angew. Chem.* **2018**, *130*, 5394–5398.
[28] M. B. Nielsen, N. Ree, K. V. Mikkelsen, M. Cacciarini, *Russ. Chem. Rev.* **2020**, *89*, 573–586.
[29] J. Daub, T. Knöchel, A. Mannschreck, *Angew. Chem. Int. Ed. Engl.* **1984**, *23*, 960–961.
[30] H. Görner, C. Fischer, S. Gierisch, J. Daub, *J. Phys. Chem.* **1993**, *97*, 4110–4117.
[31] S. L. Broman, M. Jevric, M. B. Nielsen, *Chem. Eur. J.* **2013**, *19*, 9542–9548.
[32] S. L. Broman, M. B. Nielsen, *Phys. Chem. Chem. Phys.* **2014**, *16*, 21172–21182.
[33] M. Cacciarini, A. B. Skov, M. Jevric, A. S. Hansen, J. Elm, H. G. Kjaergaard, K. V. Mikkelsen, M. B. Nielsen, *Chem. Eur. J.* **2015**, *21*, 7454–7461.
[34] M. Cacciarini, M. Jevric, J. Elm, A. U. Petersen, K. V. Mikkelsen, M. B. Nielsen, *RSC Adv.* **2016**, *6*, 49003–49010.
[35] J. Mogensen, O. Christensen, M. D. Kilde, M. Abildgaard, L. Metz, A. Kadziola, M. Jevric, K. V. Mikkelsen, M. B. Nielsen, *Eur. J. Org. Chem.* **2019**, 1986–1993.
[36] A. B. Skov, J. F. Petersen, J. Elm, B. N. Frandsen, M. Santella, M. D. Kilde, H. G. Kjaergaard, K. V. Mikkelsen, M. B. Nielsen, *ChemPhotoChem* **2017**, *1*, 206–212.
[37] A. B. Skov, N. Ree, A. S. Gertsen, P. Chabera, J. Uhlig, J. S. Lissau, L. Nucci, T. Pullerits, K. V. Mikkelsen, M. B. Nielsen, T. I. Sølling, T. Hansen, *ChemPhotoChem* **2019**, *3*, 619–629.
[38] S. L. Broman, O. Kushnir, M. Rosenberg, A. Kadziola, J. Daub, M. B. Nielsen, *Eur. J. Org. Chem.* **2015**, 4119–4130.
[39] A. B. Skov, S. L. Broman, A. S. Gertsen, J. Elm, M. Jevric, M. Cacciarini, A. Kadziola, K. V. Mikkelsen, M. B. Nielsen, *Chem. Eur. J.* **2016**, *22*, 14567–14575.
[40] A. Vlasceanu, S. L. Broman, A. S. Hansen, A. B. Skov, M. Cacciarini, A. Kadziola, H. G. Kjaergaard, K. V. Mikkelsen, M. B. Nielsen, *Chem. Eur. J.* **2016**, *22*, 10796–10800.
[41] A. Vlasceanu, B. N. Frandsen, A. B. Skov, A. S. Hansen, M. G. Rasmussen, H. G. Kjaergaard, K. V. Mikkelsen, M. B. Nielsen, *J. Org. Chem.* **2017**, *82*, 10398–10407.
[42] M. Abedi, M. Pápai, N. E. Henriksen, K. B. Møller, M. B. Nielsen, K. V. Mikkelsen, *J. Phys. Chem. C* **2019**, *123*, 25579–25584.
[43] M. Cacciarini, A. Vlasceanu, M. Jevric, M. B. Nielsen, *Chem. Commun.* **2017**, *53*, 5874–5877.
[44] Z. Wang, J. Udmark, K. Börjesson, R. Rodrigues, A. Roffey, M. Abrahamsson, M. B. Nielsen, K. Moth-Poulsen, *ChemSusChem* **2017**, *10*, 3049–3055.
[45] M. Boggio-Pasqua, M. J. Bearpark, P. A. Hunt, M. A. Robb, *J. Am. Chem. Soc.* **2002**, *124*, 1456–1470.
[46] M. Abedi, M. Pápai, K. V. Mikkelsen, N. E. Henriksen, K. B. Møller, *J. Phys. Chem. Lett.* **2019**, *10*, 3944–3949.
[47] S. T. Olsen, J. Elm, F. E. Storm, A. N. Gejl, A. S. Hansen, M. H. Hansen, J. R. Nikolajsen, M. B. Nielsen, H. G. Kjaergaard, K. V. Mikkelsen, *J. Phys. Chem. A* **2015**, *119*, 896–904.
[48] M. H. Hansen, J. Elm, S. T. Olsen, A. N. Gejl, F. E. Storm, B. N. Frandsen, A. B. Skov, M. B. Nielsen, H. G. Kjaergaard, K. V. Mikkelsen, *J. Phys. Chem. A* **2016**, *120*, 9782–9793.
[49] M. J. Kuisma, A. M. Lundin, K. Moth-Poulsen, P. Hyldgaard, P. Erhart, *J. Phys. Chem. C* **2016**, *120*, 3635–3645.
[50] M. Kuisma, A. Lundin, K. Moth-Poulsen, P. Hyldgaard, P. Erhart, *ChemSusChem* **2016**, *9*, 1786–1794.
[51] M. B. Nielsen, *ChemPhotoChem* **2019**, *3*, 168–169.
[52] *Gaussian 16* (Revision C.01), M. J. Frisch, G. W. Trucks, H. B. Schlegel, G. E. Scuseria, M. A. Robb, J. R. Cheeseman, G. Scalmani, V. Barone, G. A. Petersson, H. Nakatsuji, X. Li, M. Caricato, A. V. Marenich, J. Bloino, B. G. Janesko, R. Gomperts, B. Mennucci, H. P. Hratchian, J. V. Ortiz, A. F. Izmaylov, J. L. Sonnenberg, D. Williams-Young, F. Ding, F. Lipparini, F. Egidi, J. Goings, B. Peng, A. Petrone, T. Henderson, D. Ranasinghe, V. G. Zakrzewski, J. Gao, N. Rega, G. Zheng, W. Liang, M. Hada, M. Ehara, K. Toyota, R. Fukuda, J. Hasegawa, M. Ishida, T. Nakajima, Y. Honda, O. Kitao, H. Nakai, T. Vreven, K. Throssell, J. A. Montgomery, Jr., J. E. Peralta, F. Ogliaro, M. J. Bearpark, J. J. Heyd, E. N. Brothers, K. N. Kudin, V. N. Staroverov, T. A. Keith, R. Kobayashi, J. Normand, K. Raghavachari, A. P. Rendell, J. C. Burant, S. S. Iyengar, J. Tomasi, M. Cossi, J. M. Millam, M. Klene, C. Adamo, R. Cammi, J. W. Ochterski, R. L. Martin, K. Morokuma, O. Farkas, J. B. Foresman, D. J. Fox, Gaussian, Inc., Wallingford, CT, **2019**.
[53] C. Gonzalez, H. B. Schlegel, *J. Phys. Chem.* **1990**, *94*, 5523–5527.
[54] Y. Zhao, D. G. Truhlar, *Theor. Chem. Acc.* **2008**, *120*, 215–241.
[55] T. H. Dunning Jr., *J. Chem. Phys.* **1989**, *90*, 1007–1023.
[56] M. E. Casida, M. Huix-Rotllant, *Annu. Rev. Phys. Chem.* **2012**, *63*, 287–323.
[57] S. Mai, M. Richter, M. Heindl, M. F. S. J. Menger, A. J. Atkins, M. Ruckenbauer, F. Plasser, M. Oppel, P. Marquetand, L. González, "SHARC 2.0: Surface Hopping Including Arbitrary Couplings – Program Package for Non-Adiabatic Dynamics", can be found under http://www.sharc-md.org, **2018** (accessed 5 September 2022).
[58] S. Mai, P. Marquetand, L. González, *WIREs Comput. Mol. Sci.* **2018**, *8*, e1370.
[59] F. Neese, *WIREs Comput. Mol. Sci.* **2012**, *2*, 73–78.
[60] A. V. Marenich, C. J. Cramer, D. G. Truhlar, *J. Phys. Chem. B* **2009**, *113*, 6378–6396.
[61] T. Yanai, D. P. Tew, N. C. Handy, *Chem. Phys. Lett.* **2004**, *393*, 51–57.
[62] J.-D. Chai, M. Head-Gordon, *Phys. Chem. Chem. Phys.* **2008**, *10*, 6615–6620.
[63] E. Hernando, J. Villalva, Á. M. Martínez, I. Alonso, N. Rodríguez, R. G. Arrayás, J. C. Carretero, *ACS Catal.* **2016**, *6*, 6868–6882.
[64] J. Guilbaud, M. Laborde, H. Cattey, S. Contal, C. Montalbetti, N. Pirio, J. Roger, J.-C. Hierso, *Adv. Synth. Catal.* **2017**, *359*, 3792–3804.
[65] P. D. Legarda, A. García-Rubia, R. G. Arrayás, J. C. Carretero, *Tetrahedron* **2018**, *74*, 3947–3954.
[66] J. Corpas, M. T. Quirós, P. Mauleón, R. G. Arrayás, J. C. Carretero, *ACS Catal.* **2019**, *9*, 10567–10574.
[67] M. Martínez-Mingo, A. García-Viada, I. Alonso, N. Rodríguez, R. G. Arrayás, J. C. Carretero, *ACS Catal.* **2021**, *11*, 5310–5317.
[68] C. S. Silva, W. D. Seider, N. Lior, *Chem. Eng. Sci.* **2015**, *130*, 151–171.
[69] V. K. Mathur, *J. Econ. Educ.* **1991**, *22*, 172–178.
[70] C. Meyers, G. Rombouts, K. T. J. Loones, A. Coelho, B. U. W. Maes, *Adv. Synth. Catal.* **2008**, *350*, 465–470.
[71] K. C. Miles, C. Le, J. P. Stambuli, *Chem. Eur. J.* **2014**, *20*, 11336–11339.
[72] S. L. Broman, M. Å. Petersen, C. G. Tortzen, A. Kadziola, K. Kilså, M. B. Nielsen, *J. Am. Chem. Soc.* **2010**, *132*, 9165–9174.
[73] S. Liu, S. Cao, K. Hoang, K. L. Young, A. S. Paluch, D. L. Mobley, *J. Chem. Theory Comput.* **2016**, *12*, 1930–1941.
[74] M. A. Nedyalkova, S. Madurga, M. Tobiszewski, V. Simeonov, *J. Chem. Inf. Model.* **2019**, *59*, 2257–2263.
[75] C. Schøttler, S. K. Vegge, M. Cacciarini, M. B. Nielsen, *ChemPhotoChem* **2022**, *6*, e202200037.

Manuscript received: October 12, 2022

© 2023 The Authors. Published by Wiley-VCH GmbH

26289725, 0, Downloaded from https://chemistry-europe.onlinelibrary.wiley.com/doi/10.1002/cmtd.202200060 by Linkoping Universitet, Wiley Online Library on [03/04/2023]. See the Terms and Conditions (https://onlinelibrary.wiley.com/terms-and-conditions) on Wiley Online Library for rules of use; OA articles are governed by the applicable Creative Commons License

RESEARCH ARTICLE

Most out of MOST: A major challenge in the development of molecular solar thermal energy (MOST) systems is that many and often conflicting performance criteria need to be met by one single molecule. Here an original computational approach is introduced to address this challenge and is used to identify several dihydroazulene/vinylheptafulvene compounds with excellent overall properties for future MOST applications.

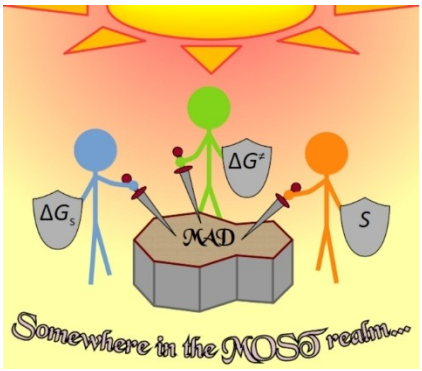

Dr. E. M. Arpa, Prof. B. Durbeej**

26289725, 0, Downloaded from https://chemistry-europe.onlinelibrary.wiley.com/doi/10.1002/cmtd.202200060 by Linkoping Universitet, Wiley Online Library on [03/04/2023]. See the Terms and Conditions (https://onlinelibrary.wiley.com/terms-and-conditions) on Wiley Online Library for rules of use; OA articles are governed by the applicable Creative Commons License